

# Infrared defect dynamics—Nitrogen-vacancy complexes in float zone grown silicon introduced by electron irradiation

Naohisa Inoue<sup>1,2,a)</sup> and Yuichi Kawamura<sup>2</sup>

<sup>1</sup>Tokyo University of Agriculture and Technology, 2-24-16, Naka-cho, Koganei, Tokyo 184-8588, Japan

<sup>2</sup>Osaka Prefecture University, 1-2, Gakuen-cho, Naka-ku, Sakai, Osaka 599-8570, Japan

(Received 31 October 2017; accepted 18 April 2018; published online 8 May 2018)

The interaction of nitrogen and intrinsic point defects, vacancy (V) and self-interstitial (I), was examined by infrared absorption spectroscopy on the electron irradiated and post-annealed nitrogen doped float zone (FZ) silicon crystal. Various absorption lines were observed, at  $551\text{ cm}^{-1}$  in as-grown samples, at  $726$  and  $778\text{ cm}^{-1}$  in as-irradiated samples (Ir group), at  $689\text{ cm}^{-1}$  after post-annealing at  $400^\circ\text{C}$  and above ( $400^\circ\text{C}$  group), at  $762$  and  $951\text{ cm}^{-1}$  after annealing at  $600^\circ\text{C}$  ( $600^\circ\text{C}$  group), and at  $714\text{ cm}^{-1}$  up to  $800^\circ\text{C}$  ( $800^\circ\text{C}$  group). By irradiation, a part of  $\text{N}_2$  was changed into the Ir group.  $\text{VN}_2$  is the candidate for the origin of the Ir group. By the post annealing at  $400$  and  $600^\circ\text{C}$ , a part of  $\text{N}_2$  and the Ir group were changed into the  $400^\circ\text{C}$  group, to less extent at  $600^\circ\text{C}$ .  $\text{V}_2\text{N}_2$  is the candidate for the origin of the  $400^\circ\text{C}$  group. By annealing at  $600^\circ\text{C}$ , most of the Ir group turned into  $400^\circ\text{C}$  and  $600^\circ\text{C}$  groups. By annealing at  $800^\circ\text{C}$ ,  $\text{N}_2$  recovered almost completely, and most other complexes were not observed. Recently, lifetime degradation has been observed in the nitrogen doped FZ Si annealed at between  $450$  and  $800^\circ\text{C}$ . The N-V interaction in the same temperature range revealed here will help to understand the lifetime degradation mechanism. The behavior of the  $689\text{ cm}^{-1}$  line corresponded well to the lifetime degradation. *Published by AIP Publishing.*

<https://doi.org/10.1063/1.5011224>

## I. INTRODUCTION

Nitrogen doping in silicon crystals was widely used to suppress grown-in microdefects in 1995.<sup>1</sup> The interaction between N and intrinsic point defects of both vacancies (V) and self-interstitials (I) at high temperature plays an important role in suppressing the defect formation during cooling after crystal growth. It is difficult, however, to experimentally examine such a high temperature process. Moreover the N, V, and I concentrations are so low that it is hard to experimentally examine their behavior even at room temperature. We thought that by electron irradiation, we could introduce enough point defects and that by highly sensitive infrared absorption (IR) spectroscopy, we could systematically and quantitatively analyze their behavior.<sup>2</sup> The IR study of nitrogen and its complex with point defects had been experimentally done on the N ion implantation process for forming buried thin films in devices in the 1980s.<sup>3</sup> Theoretical studies had been done considering the grown-in defect formation in the N doped crystal in the 2000s,<sup>4</sup> but the accompanying experiments had only been done on the N implanted samples.

On the other hand, radiation induced oxygen-carbon—V—I—complexes had been studied by IR for a long time.<sup>5</sup> In 2004, radiation induced  $\text{C}_i\text{O}_i$  (interstitial pair) was used as a lifetime killer in the power device for the hybrid cars.<sup>6</sup> The carbon concentration and the irradiation dose used for the simulation of such an application were  $1 \times 10^{16}\text{ atoms cm}^{-3}$  and  $3 \times 10^{17}\text{ electrons cm}^{-2}$  at maxima.<sup>2,7</sup> These were

2 and 1 orders of magnitude lower, respectively, than those in the previous studies.<sup>5</sup> We studied the behavior of the complexes including  $\text{C}_i\text{O}_i$  by developing highly sensitive, systematic, and quantitative IR (infrared defect dynamics<sup>7</sup>). More than 30 absorption lines from about 20 complexes were measured<sup>8</sup> for the complex concentration down to  $10^{12}\text{ cm}^{-3}$ .

There had never been IR studies on the electron irradiation of the N doped crystal. The N-doped crystal is used for power devices now. Then, we have started the irradiation study on both nitrogen doped Czochralski (NCZ) and nitrogen doped FZ (NFZ) Si crystals.<sup>9</sup> By the electron irradiation, loss of  $\text{N}_2$  was found in the NFZ Si crystals.<sup>10</sup> Correspondingly, the new absorption lines appeared after irradiation and post-annealing.<sup>10</sup> A few lines were assigned to be from  $\text{VN}_2$ .<sup>10</sup> In the same study, the absorption line at  $551\text{ cm}^{-1}$  was observed in the as-grown crystal and suggested to be due to  $\text{N}_s$ .<sup>11</sup> Here, we continue the study on these complexes.

Recently, the lifetime degradation has been observed after annealing of NFZ silicon.<sup>12</sup> The N interaction with V was suggested to be related to the degradation.<sup>13</sup> We discuss the relationship between the complex behavior and the lifetime behavior here. We examined NCZ silicon also, but the  $\text{N}_2$  loss and complex behavior observed in the NFZ crystal were not observed.<sup>10</sup> Recently, a similar IR study of NCZ silicon has been reported for high electron dose.<sup>14</sup> Some results agreed with our results, but there were some differences. We discuss them also here.

## II. EXPERIMENTAL

Samples were NFZ silicon single crystals. The [N] (nitrogen concentration), [C], and [O] were determined by

Note: This paper is part of the Special Topic section “Defects in Semiconductors 2017” published in Journal of Applied Physics April 28, Volume 123 Issue 16 (2018).

<sup>a)</sup>Author to whom correspondence should be addressed: inouen@riast.osakafu-u.ac.jp

the IR measurement as summarized in Table I. Two nitrogen concentration levels (named p and k) from 2 crystals (No. 5 and No. 2) were examined. The result of the highest [N] sample 5p is mainly shown here. They were almost undoped. The samples were finished to be about 1 cm  $\times$  1 cm in size and 2 mm in thickness, and both surfaces were mirror polished. Electron irradiation was done at room temperature at Takasaki Advanced Radiation Research Institute. The electron acceleration energy was 2 MeV, and the dose was from  $1 \times 10^{15}$  to  $1 \times 10^{17}$  cm $^{-2}$ . The samples were water cooled from the back side during irradiation so that the sample temperature was kept below 150 °C for the case of  $1 \times 10^{17}$  cm $^{-2}$  dose. The annealing was done at 200, 400, 600, and 800 °C for 10 min. As will be shown later, there were differences between the spectra of the as-irradiated sample and the sample annealed at 200 °C.

The infrared absorption measurement was done at room temperature. The wavenumber resolution was 2 cm $^{-1}$ , but for low concentration complexes, 4 cm $^{-1}$  was employed also to improve the S/N ratio. The sensitivity of the absorption line was in the  $10^{-6}$  peak absorbance (A) range at best. The peak absorbance was estimated by fitting the Lorentzian function to each absorption peak (see JEITA EM3512 described later). The baselines to the peaks were created by subtracting the Lorentzian function of adequate size from the spectrum. The baselines will be shown in Figs. 2, 3, and 5(a) and 5(b). In this paper, the peak absorbance is used in the discussion for simplicity. The concentration of most complexes can be roughly estimated by multiplying the peak absorbance by  $10^{18}$  times as follows: The absorption coefficient (defined for 1 cm thickness) is obtained from the absorbance in the 2 mm thick sample by multiplying 10 [=log 10/log e (=2.303)  $\times$  the thickness ratio of 10 mm for the absorption coefficient/sample thickness of 2 mm (=5)]. The conversion coefficients from the absorption coefficient of the dominant absorption line to the impurity concentrations are 1.82, 0.82, and  $3.13 \times 10^{17}$  cm $^{-2}$  for nitrogen, carbon, and oxygen, respectively, as given in the SEMI and JEITA standard measurement procedures JEITA EM3512, SEMI MF1391, and SEMI MF1188, respectively. This shows that the dipole moments of representative local vibrational modes (LVM) of N, C, and O are within a factor of 4. We estimated the relative dipole moments of the dominant C and O containing complexes and made the tentative database in Ref. 11. This database made it possible to quantitatively analyze complexes in terms of the concentration rather than the absorbance. Previously, we have determined the relative dipole moments of 963 (N $_2$ ), 996 (N $_2$ O), and 810 (N $_2$ O $_2$ ) cm $^{-1}$  lines theoretically and experimentally to be 1:1/1.5:1/0.5 as adopted in JEITA EM3512. We have not estimated the relative dipole

TABLE I. Nitrogen, carbon, and oxygen concentrations of the samples (atoms cm $^{-3}$ ).

Sample	[N] $10^{15}$	[C] $10^{15}$	[O] $10^{16}$
5p	7.9	2	2
5k	0.5	2	2
2p	3.6	2	1
2k	0.4	2	1

moment of other nitrogen containing complexes yet. Therefore, we discuss using the absorbance here.

### III. COMPLEXES IN AS-GROWN NFZ SILICON

In addition to the well-known absorption lines from N $_2$  at 766 (appeared at 766.8 cm $^{-1}$  here but IR machine dependent) and 963 (963.6) cm $^{-1}$ , the absorption line was observed at 551 cm $^{-1}$  (550.6) as shown in Fig. 1. This line had been observed after the N ion implantation and laser and furnace annealing<sup>3</sup> but had not been observed in the as-grown crystal yet. In the ion implantation study, the 653 cm $^{-1}$  line had been observed more clearly than the 551 cm $^{-1}$  line after laser annealing and assigned to be due to N $_s$ .<sup>3</sup> N $_s$  had been observed by the electron paramagnetic resonance (EPR) study on the ion implanted and laser annealed sample and called as SL5.<sup>15</sup> In that paper,<sup>3</sup> the 551 cm $^{-1}$  line was suggested to be related to N $_s$ , but it was said that the 551 cm $^{-1}$  line was developed by the furnace annealing which was not the case of SL5 and 653 cm $^{-1}$  line. As seen from the spectra in Fig. 1, the absorbance of the 551 cm $^{-1}$  line was proportional to that of the N $_2$  766 and 963 cm $^{-1}$  absorption lines. In this case, it was about 1/3 of the N $_2$  line absorbance. It is important to clarify the origin. There was a strong absorption line at 668 cm $^{-1}$  in as grown nitrogen doped Si crystals also (both CZ and FZ).

### IV. ABSORPTION LINES APPEARING UPON IRRADIATION

Figure 2 shows an example of the differential absorption spectra between 700 and 850 cm $^{-1}$  of the NFZ silicon **after irradiation and annealing using the non-irradiated sample as the reference**. The loss of N $_2$  absorption at 766 cm $^{-1}$  is indicated by drawing the baseline by fitting the Lorentzian function to the peak. The strong absorption lines at 726 (726.3) and 778 (778.4) cm $^{-1}$  appeared as already reported.<sup>10</sup> The 726 cm $^{-1}$  absorption line was a little weaker but wider than the 778 cm $^{-1}$  line. Their peak absorbances were comparable to the loss of the N $_2$  766 cm $^{-1}$  line peak absorbance. This suggests that N $_2$  turned into some structure which made these

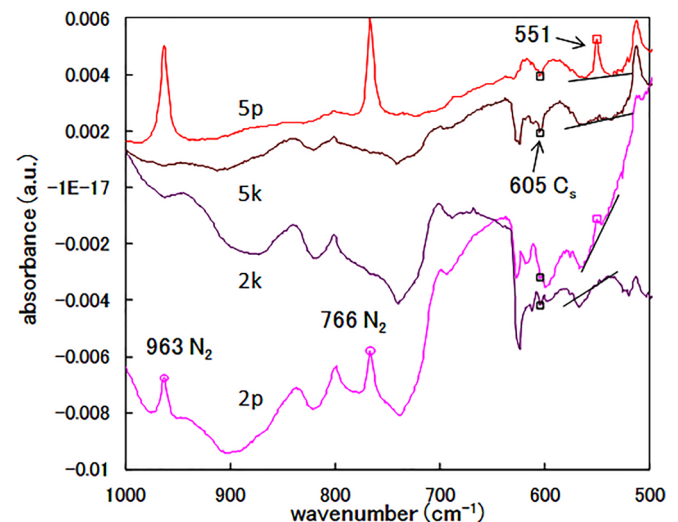


FIG. 1. Absorption line at 551 cm $^{-1}$  in as-grown NFZ silicon compared to N $_2$  absorption lines at 766 and 963 cm $^{-1}$ .

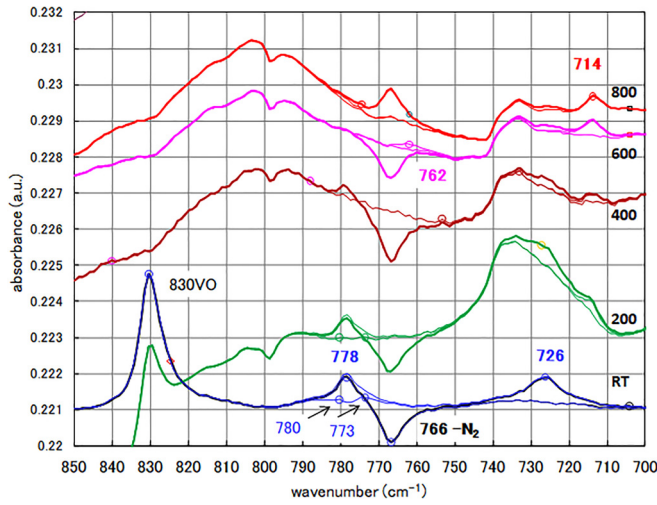


FIG. 2. Differential absorption spectra between 700 and 850  $\text{cm}^{-1}$  after irradiation and annealing at 200, 400, 600, and 800  $^{\circ}\text{C}$ . Absorption lines at 778, 726, 762, and 714  $\text{cm}^{-1}$  were observed distinctly. Baselines were created by fitting the Lorentz function to the individual absorption line. The electron dose was  $1 \times 10^{17}/\text{cm}^2$ .

absorption lines. We call the 726 and 778  $\text{cm}^{-1}$  absorption lines the “Ir” radiation group. The nitrogen-related absorption lines observed in this study are summarized in Table II.

There were many other well-known absorption lines from  $\text{O}_i$  (514; 514.1, 1107), VO (830; 830.4),  $\text{C}_i\text{O}_i$  (525.7, 537.2, 545.9, 862; 862.3),  $\text{VO}^-$  (889, 889.3),  $\text{IC}_i\text{O}_i$  (936, 936.5 and 1020, 1020.4),  $\text{I}_3\text{C}_i\text{O}_i$  (988, 988.6),  $\text{I}_2\text{C}_i\text{O}_i$  (994, 994.2), and  $\text{C}_s\text{O}_{2i}$  (1047, 1047.4  $\text{cm}^{-1}$ ) in the irradiated sample 5p. These CO complexes are characteristic of the so-called “C-rich” samples.<sup>16</sup> Self-interstitial replaces substitutional carbon  $\text{C}_s$  to emit interstitial carbon  $\text{C}_i$ .  $\text{C}_i$  then forms various CO complexes. When the sample is C-rich, most of the I is consumed by C and V is superior to I. In sample 2p, in addition to the above C-rich complex lines,  $\text{I}_2\text{O}_{2i}$  (916, 916.2) and  $\text{IO}_{2i}$  (922, 922.9  $\text{cm}^{-1}$ ) lines were observed. These are the characteristic of the so-called “C-lean” condition in low [C] samples<sup>17</sup> where I also plays an important role. We call this mixed condition the “C-medium.” These suggest that  $\text{N}_2$  reacted with V rather than with I in sample 5p. As shown later, there were some differences in the complex behavior between samples 5p and 2p. There was no

TABLE II. Absorption lines observed in this study: the peak wavenumber ( $\text{cm}^{-1}$ ), state or temperature where they were dominant, full width at half maximum of the fitted Lorentz function ( $\text{cm}^{-1}$ ), and candidate of the complex of the origin of absorption. In addition to those listed in table, there were weak absorption lines at 961, 773, and 780  $\text{cm}^{-1}$  (see Sec. VIE).

$\text{cm}^{-1}$	Dominant	FWHM	Origin
766	As-grown	7	$\text{N}_2$
963	As-grown	10	$\text{N}_2$
726	As-irradiated	10	$\text{VN}_2$
778	As-irradiated	6	$\text{VN}_2$
689	400 (200–600) $^{\circ}\text{C}$	9	$\text{V}_2\text{N}_2$
762	600 $^{\circ}\text{C}$	7	?
951	600 $^{\circ}\text{C}$	7	?
714	800 $^{\circ}\text{C}$ (200 $^{\circ}\text{C}$ )	5	?
551	As-grown	5	?

distinct difference in [C] between crystal 5 and crystal 2. [O] might be related to the complex behavior.

Figure 3 shows the spectra between 530 and 630  $\text{cm}^{-1}$ . The loss of 605  $\text{cm}^{-1}$  ( $\text{C}_s$ ) and 551  $\text{cm}^{-1}$  absorption lines by the irradiation was observed as in the case of 766 and 963  $\text{cm}^{-1}$  lines ( $\text{N}_2$ ) shown in Figs. 2 and 5(b).

## V. ANNEALING TEMPERATURE DEPENDENCE OF THE NEW ABSORPTION LINES

### A. 200 $^{\circ}\text{C}$

No new peaks appeared by the annealing at 200  $^{\circ}\text{C}$ . (There was no “200  $^{\circ}\text{C}$  group.”) Figure 2 shows the annealing temperature dependence of the peaks at 726 and 778  $\text{cm}^{-1}$ . They were strong after irradiation but reduced monotonously after annealing at 200, 400, and 600  $^{\circ}\text{C}$  and disappeared upon annealing at 800  $^{\circ}\text{C}$  as summarized in Fig. 4. The temperature dependences of the two lines were nearly equal to each other (within the experimental accuracy). The VO absorption line at 830  $\text{cm}^{-1}$  reduced to about half by the annealing at 200  $^{\circ}\text{C}$ . This showed that a half of VO breaks into V and O which could react with other complexes. This was in contrast to VO turned into  $\text{VO}_n$  ( $n = 2, 3, \dots$ ) in the case of NCZ Si.<sup>16,17</sup>

### B. 400 $^{\circ}\text{C}$

Absorption lines at 726 and 778  $\text{cm}^{-1}$  were only weakly observed after the annealing at 400  $^{\circ}\text{C}$ . A new strong peak appeared at 689 (688.7)  $\text{cm}^{-1}$  upon the annealing at 400  $^{\circ}\text{C}$ . Figure 5(a) shows the annealing temperature dependence of the 689  $\text{cm}^{-1}$  absorption line. It was big after annealing at 400  $^{\circ}\text{C}$  but weak at 600  $^{\circ}\text{C}$ , weaker at 200  $^{\circ}\text{C}$ , and not confirmed well at 800  $^{\circ}\text{C}$  nor as-irradiated. Thus, we call the origin of this line the “400  $^{\circ}\text{C}$  group.” The full width at half maximum of the 689  $\text{cm}^{-1}$  line was large, considering that the peak wavenumber was low. Overlapping of neighboring absorption lines was suggested in sample 2p. As seen in Figs. 2 and 4, 726 and 778  $\text{cm}^{-1}$  absorption lines (“Ir” group) were weakened, and the loss of the 766  $\text{cm}^{-1}$  line increased by the annealing at 400  $^{\circ}\text{C}$  compared to those after irradiation. These suggested

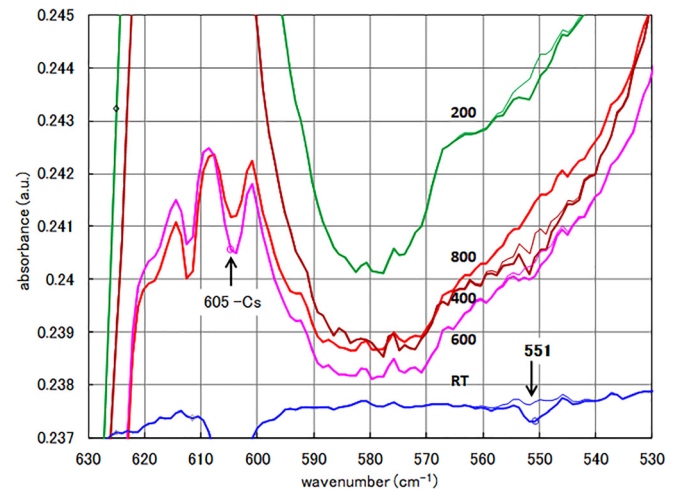


FIG. 3. Differential absorption spectra between 530 and 630  $\text{cm}^{-1}$  after irradiation and annealing. Negative absorption was observed in 605  $\text{cm}^{-1}$  ( $\text{C}_s$ ) and 551  $\text{cm}^{-1}$  lines.



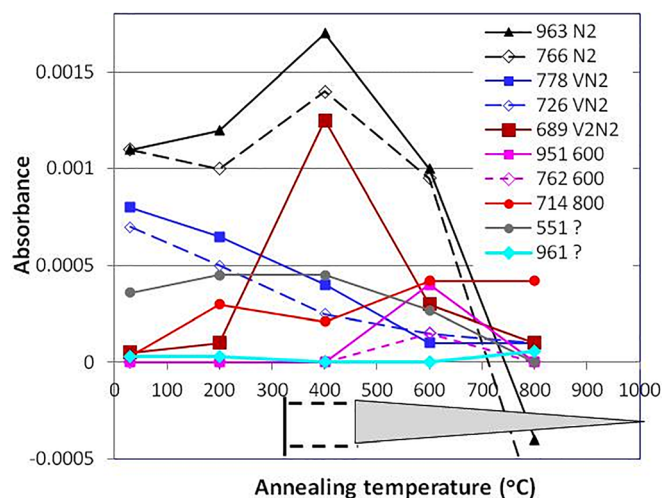


FIG. 4. Post annealing temperature dependence of the peak absorbances of the various absorption lines. Lifetime degradation was reported for the annealing temperature range indicated by the gray triangle and the vertical and horizontal lines in the bottom.

that a part of  $N_2$  and the Ir group changed into the  $400^\circ\text{C}$  group by the annealing at  $400^\circ\text{C}$  (and  $600$  and  $200^\circ\text{C}$ ). In other words, the conversion of  $N_2$  and the Ir group to the  $400^\circ\text{C}$  group took place much at  $400^\circ\text{C}$ , less at  $600^\circ\text{C}$ , and a little at  $200^\circ\text{C}$ . The VO absorption line disappeared after annealing at  $400$  (and  $600$  and  $800^\circ\text{C}$ ). V and O could react with other complexes at these temperatures also. In Fig. 3, it is shown that the loss of the  $551\text{ cm}^{-1}$  line slightly increased upon annealing at  $400^\circ\text{C}$  and disappeared at  $800^\circ\text{C}$ , similar to the loss of  $N_2$  absorption lines, as summarized in Fig. 4.

### C. $600^\circ\text{C}$

The absorption lines at  $726$  and  $778\text{ cm}^{-1}$  were hardly observed after annealing at  $600^\circ\text{C}$ . The loss of  $N_2$  lines was reduced a little compared to that after the irradiation. The  $689\text{ cm}^{-1}$  absorption line was observed much weaker than that after annealing at  $400^\circ\text{C}$ . Therefore, a part of the Ir group introduced by the irradiation returned to  $N_2$  by the annealing at  $600^\circ\text{C}$ .

The new line at  $714$  ( $713.7$ )  $\text{cm}^{-1}$  was distinct after annealing at  $600^\circ\text{C}$  as observed in Fig. 2. In a detailed examination, this  $714\text{ cm}^{-1}$  absorption line was observed after annealing at  $200$ ,  $400$ , and  $800^\circ\text{C}$  as shown in Fig. 2. We call this the “ $800^\circ\text{C}$ ” group. In sample 2p, this line was faintly observed after irradiation also.

A new weak absorption was observed at  $762$  ( $762.0$ )  $\text{cm}^{-1}$  close to the  $766\text{ cm}^{-1}$   $N_2$  peak after annealing at  $600^\circ\text{C}$  as shown in Fig. 2. The peak at  $951$  ( $951.0$ )  $\text{cm}^{-1}$  close to the  $963\text{ cm}^{-1}$  absorption line was also observed as shown in Fig. 5(b). They were not observed clearly after the annealing at other temperatures. We call them the “ $600^\circ\text{C}$ ” group.

### D. $800^\circ\text{C}$

The  $N_2$  absorption line at  $766$  (and  $963$ )  $\text{cm}^{-1}$  was recovered by the annealing at  $800^\circ\text{C}$ . In Figs. 2 and 5(b), it is shown that  $N_2$  absorption was bigger after annealing at  $800^\circ\text{C}$

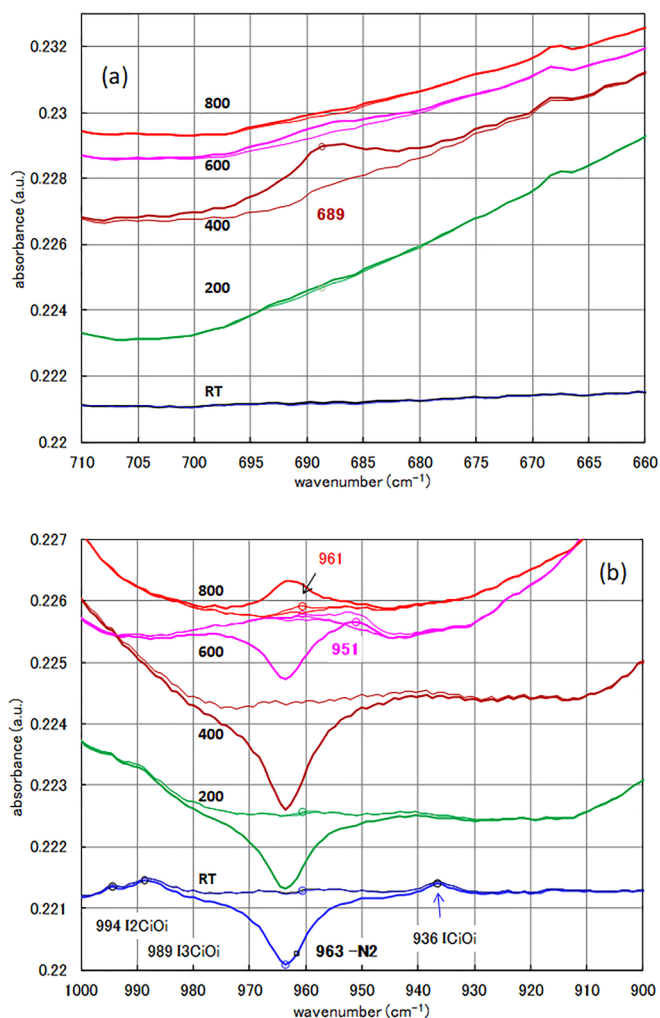


FIG. 5. Differential absorption spectra after irradiation and annealing. (a) Peak at  $689\text{ cm}^{-1}$ . (b)  $963\text{ cm}^{-1}$   $N_2$  line and the accompanying lines.  $C_iO_i$  related complexes are also shown.

than that in the as-grown sample in the case of the sample 5p. This is interpreted that  $N_s$  (and possibly the other structure,  $N_i$ ) was present in the as-grown sample and formed  $N_2$  by the irradiation and annealing at  $800^\circ\text{C}$ . This phenomenon was not distinct in sample 2p. This difference might also be related to the C-rich character of sample 5p and C-medium character of sample 2p. We have not understood the mechanism yet.

## VI. DISCUSSION

### A. $726$ and $778\text{ cm}^{-1}$ absorption lines (Ir group, $VN_2$ )

We have previously assigned these lines to be due to  $VN_2$ , a modified structure from  $N_2$  considering the following characters: (1) They appeared near the  $766\text{ cm}^{-1}$  ( $N_2$ ) absorption line and corresponded to the decrease in  $N_2$  so that their origin was likely to be a slight modification of  $N_2$ .<sup>10,11</sup> (2) The intensity of these lines was comparable to the loss of  $N_2$  lines. This suggested that their origin had a similar structure to  $N_2$ . We add more character here: (3) Sample 5p was V-rich, as suggested from the presence of V-type CO complexes. In the C-rich material, most I was consumed by the formation of  $I_nC_iO_i$  ( $n = 1-3$ )<sup>16</sup> observed here. [On the other hand, in C-lean samples,  $I_mO_n$  ( $m = 1-2$  and  $n = 1-3$ ) were

dominant.<sup>17]</sup> They were observed in addition to  $I_nC_iO_i$  in the sample 2p. (4) Many vacancies were supplied in FZ silicon because VO breaks by the annealing at 400 °C (and at 600 and 800 °C and less at 200 °C) as seen from Fig. 2 and emits free V, in contrast to form  $VO_n$  ( $n > 1$ ) in the case of CZ Si.<sup>17</sup>

$VN_2$  was theoretically examined by Sawada and Kawakami,<sup>18</sup> Kageshima *et al.*,<sup>19</sup> and Goss *et al.*<sup>20</sup> who examined the IR absorption experimentally also. It has two structures. One is composed of two N-Si<sub>2</sub>N connected at N (D2d symmetry). The calculated LVM frequencies<sup>20</sup> were 774.1 and 573.4 cm<sup>-1</sup>. The other structure is N<sub>s</sub>-N<sub>i</sub> or the combination of nonplanar NSi<sub>3</sub> (NH<sub>3</sub> type, the source of the 963 cm<sup>-1</sup> absorption line in the case of N<sub>2</sub>) and NSi<sub>2</sub> (H<sub>2</sub>O type, the source of the 766 cm<sup>-1</sup> absorption line in the case of N<sub>2</sub>). The latter has a little higher energy than the former. The calculated LVM frequencies<sup>20</sup> were 1163.1, 672.8, and 592.8 cm<sup>-1</sup>.

Absorption lines at 782 and 790 cm<sup>-1</sup> had been described by Goss<sup>20</sup> without referring to the data and detailed discussion. He suggested them to correspond to the theoretically predicted absorption by  $VN_2$  at 774.1 cm<sup>-1</sup>. The 782 cm<sup>-1</sup> line location at low temperature is close to that of our 778 cm<sup>-1</sup> line at room temperature. Sgourou *et al.*<sup>14</sup> have recently observed 726 and 778 cm<sup>-1</sup> lines in the irradiated NCZ Si and followed our assignment as  $VN_2$ . Karoui and Karoui<sup>21</sup> related the described 782 and 790 cm<sup>-1</sup> lines to their theoretical result of  $VN_2$  at 781 cm<sup>-1</sup>. Thus, our assignment was supported by the various works.

### B. 689 cm<sup>-1</sup> absorption line (400 °C group, $V_2N_2$ )

There had never been the report on the 689 cm<sup>-1</sup> absorption line. Stein reported the similar absorption line at 687 cm<sup>-1</sup> in the implanted (and annealed at 350 °C) samples<sup>22</sup> but not assigned. In addition, the same author later observed 967, 771, 691, and 658 cm<sup>-1</sup> absorption lines and suggested the 691 cm<sup>-1</sup> line due to N<sub>i</sub>.<sup>23</sup> Goss<sup>20</sup> described that Stein had associated the 690 cm<sup>-1</sup> absorption line with N<sub>i</sub>, but for him, this wavenumber seemed too low for N<sub>i</sub>, and he assigned it to  $VN_s$  which was predicted at 663 cm<sup>-1</sup>.

However, we have previously proposed  $V_2N_2$  for the origin of the 689 cm<sup>-1</sup> absorption line.<sup>11</sup> The reasons are discussed in detail here. (1) It is natural that  $VN_2$  turns into  $V_2N_2$  when enough V is provided by the annealing. (2) V was supplied by the break of VO by the annealing. (3)  $V_2N_2$  had been examined theoretically also<sup>18–20</sup> and had been considered to be most stable under V-rich conditions. (4) This line appeared upon annealing at 400 °C instead of the weakened 726 and 778 cm<sup>-1</sup>  $VN_2$  lines. Therefore, this line is likely to emit from the configuration modified from  $VN_2$ . (5) The intensity of the 689 cm<sup>-1</sup> absorption line corresponded well to the loss of N<sub>2</sub> lines. These features were like those of N<sub>2</sub> and the Ir group after irradiation, resulting in the formation of  $VN_2$ . (6) The theoretical study<sup>20</sup> predicted the absorption line of  $V_2N_2$  at 668 cm<sup>-1</sup> which is not so far from 689 cm<sup>-1</sup>. The  $V_2N_2$  structure (D3d symmetry) is two NSi<sub>3</sub> components lying parallel and facing with each other.<sup>4</sup>

### C. 762 and 951 cm<sup>-1</sup> absorption lines (600 °C group)

There had never been a report on such absorption lines. Sgourou observed the 953 cm<sup>-1</sup> line in the electron irradiated NCZ silicon and attributed it to  $IN_2$ .<sup>14</sup>  $IN_2$  is I-oriented or expected to be observed in the C-lean sample so that it is unlikely in sample 5p which was enough of V. The origin is not clear yet. There are nitrogen monomers such as N<sub>s</sub>, N<sub>i</sub>, and  $VN_s$ . We do not have enough information to discuss them yet.

### D. 714 cm<sup>-1</sup> absorption line (800 °C group)

There had been no observation of such a line. This line was observed after annealing between 200 and 800 °C, the highest temperature among the complexes. There was a small signal of the 714 cm<sup>-1</sup> line in the as-irradiated sample 2p, but we could not detect it in the as-irradiated sample 5p as shown in Fig. 2. This might be related to the C-rich and C-medium natures of samples 5p and 2p, respectively. The mechanism is not clear yet also.

### E. 551 cm<sup>-1</sup> absorption line and others

In the recent study of irradiation and annealing of NCZ Si, the absorption line at 653 cm<sup>-1</sup> (N<sub>s</sub>) has been observed, but the spectra below 630 cm<sup>-1</sup> were not reported.<sup>14</sup> On the contrary, in our study, the 653 cm<sup>-1</sup> line was not observed, and it is not clear why such discrepancy occurred. The 551 cm<sup>-1</sup> absorption line was weakened by the irradiation, and its loss slightly increased by the annealing at 400 °C and almost recovered by the annealing at 800 °C.

There were other new absorption lines observed with a small signal, for example, the line at 961 cm<sup>-1</sup> [960.6 cm<sup>-1</sup> in Figs. 5(b) and 4, mainly at 800 °C] and the lines at 773 and 780 cm<sup>-1</sup> (773.5 and 780.3 cm<sup>-1</sup> in Fig. 2, RT and 200 °C). We will report them in the future.

### F. Comparison to NCZ silicon

We have studied the annealing behavior of irradiated NCZ silicon. Neither a decrease in N<sub>2</sub> nor radiation induced complexes were observed.<sup>24</sup> There has been a study on irradiated NCZ silicon recently.<sup>14</sup> The authors observed some radiation induced absorption lines, probably due to the higher dose they employed than ours. The authors followed our assignment of  $VN_2$  for 726 and 778 cm<sup>-1</sup> absorption lines. They assigned the 953 cm<sup>-1</sup> line to be due to  $IN_2$ . This was close to our 951 cm<sup>-1</sup> absorption line of the 600 °C group. Our sample 5p was V-rich so that the complex contained V rather than I. More detail on the complexes in NCZ silicon after irradiation and annealing will be discussed in a separate paper.

### G. Relation to the lifetime degradation in annealed NFZ silicon

Recently, the carrier lifetime degradation has been reported in the annealed NFZ silicon.<sup>12</sup> The lifetime was the shortest between 450 and 600 °C, short at 700 °C, and slightly short at 800 °C. No change was observed at 300 °C and above 1000 °C. The result is indicated by the lines and the triangle

in the bottom of Fig. 4 for comparison to our result. This temperature range was nearly the same as that where the big change in the radiation induced complex took place in the present study. Especially, the  $689\text{ cm}^{-1}$  line ( $\text{V}_2\text{N}_2$  related) was observed after annealing at  $400^\circ\text{C}$  and  $600^\circ\text{C}$ . The strong lifetime shortening took place around there. The 726 and  $778\text{ cm}^{-1}$  absorption lines ( $\text{VN}_2$ ) were observed after irradiation and remained after annealing mainly at  $200\text{--}400^\circ\text{C}$ . Lifetime degradation, however, was not observed after annealing at  $200^\circ\text{C}$ . Unfortunately, they lack the data at  $400^\circ\text{C}$ , and our data are absent for  $500^\circ\text{C}$ . The origin of the  $689\text{ cm}^{-1}$  absorption line assigned as  $\text{V}_2\text{N}_2$  looks most closely related to the lifetime degradation. The author of that paper suggested that  $\text{N}_2\text{-V}$  reaction might take place.<sup>13</sup> The result in the present study suggested the lifetime degradation mechanism of annealed NFZ silicon.

## VII. CONCLUSION

In summary, various absorption lines were observed, at  $551\text{ cm}^{-1}$  in as-grown samples, at 726 and  $778\text{ cm}^{-1}$  in as-irradiated samples (Ir group), at  $689\text{ cm}^{-1}$  after post-annealing at  $400^\circ\text{C}$  and above ( $400^\circ\text{C}$  group), at 762 and  $951\text{ cm}^{-1}$  after annealing at  $600^\circ\text{C}$  ( $600^\circ\text{C}$  group), and at  $714\text{ cm}^{-1}$  up to  $800^\circ\text{C}$  ( $800^\circ\text{C}$  group). By irradiation, a part of  $\text{N}_2$  turned into the Ir group, probably  $\text{VN}_2$ . By the post annealing at  $400$  and  $600^\circ\text{C}$ ,  $\text{N}_2$  and the Ir group ( $\text{VN}_2$ ) turned into the  $400^\circ\text{C}$  group, probably  $\text{V}_2\text{N}_2$ . By annealing at  $800^\circ\text{C}$ ,  $\text{N}_2$  recovered almost completely, and most other complexes were not observed. Recently, lifetime degradation has been observed in the NFZ sample annealed between  $450$  and  $800^\circ\text{C}$ . The  $\text{N-V}$  interaction in the same temperature range revealed here helps to understand the lifetime degradation mechanism. Infrared defect dynamics is the powerful tool to analyze the defects in science and technology.

## ACKNOWLEDGMENTS

The authors are grateful to H. Hanaya (JAEA) for irradiation and L. I. Murin (ISSSP, Belarus), B. G. Svensson (U. Oslo), V. P. Markevich (U. Manchester), C. A. Londos (U. Athens), R. Jones (U. Exeter), and H. Ch. Alt (U. Applied Science, Germany) for discussion.

- <sup>1</sup>T. Abe, H. Harada, N. Ozawa, and K. Adomi, "Deep level generation-annihilation in nitrogen doped FZ crystals," in *Oxygen, Carbon, Hydrogen, and Nitrogen in Crystalline Silicon*, edited by J. C. Mikkelsen, Jr., S. J. Pearton, J. W. Corbett, and S. J. Pennycook (Mater. Res. Soc. Symp. Proc., Boston, 1986), Vol. 59, p. 537.
- <sup>2</sup>N. Inoue, H. Ohyama, Y. Goto, and T. Sugiyama, *Physica B* **401–402**, 477 (2007).
- <sup>3</sup>H. J. Stein, *Appl. Phys. Lett.* **43**, 296 (1983).
- <sup>4</sup>R. Jones, I. Hahn, J. P. Goss, P. R. Briddon, and S. Öberg, *Solid State Phenom.* **95–96**, 93 (2003).
- <sup>5</sup>L. I. Murin, V. P. Markevich, J. L. Lindstroem, M. Kleverman, J. Hermansson, T. Hallberg, and B. G. Svensson, *Solid State Phenom.* **82–84**, 57 (2002).
- <sup>6</sup>T. Sugiyama, S. Yamazaki, S. Nakagaki, and M. Ishiko, in *Proceedings of the 17th International Symposium on Power Semiconductor Devices & ICs*, Santa Barbara (2004), p. 243.
- <sup>7</sup>N. Inoue, Y. Goto, T. Sugiyama, S. Yamazaki, and T. Kushida, in *Proceedings of the High Purity Silicon IX* (2006), p. 313.
- <sup>8</sup>N. Inoue, Y. Goto, T. Sugiyama, K. Watanabe, H. Seki, and Y. Kawamura, *Phys. Status Solidi B* **251**, 2205 (2014).
- <sup>9</sup>N. Inoue, S. Shirafuji, H. Ohyama, Y. Goto, T. Sugiyama, and H. Ono, in *Proceedings of the Forum Science and Technology of Silicon Materials*, Niigata (2007), p. 12.
- <sup>10</sup>N. Inoue, H. Oyama, K. Watanabe, H. Seki, and Y. Kawamura, *AIP Conf. Proc.* **1583**, 19 (2014).
- <sup>11</sup>N. Inoue, T. Sugiyama, Y. Goto, K. Watanabe, H. Seki, and Y. Kawamura, *Phys. Status Solidi C* **13**, 833 (2016).
- <sup>12</sup>N. E. Grant, V. P. Markevich, J. Mullins, A. R. Peaker, F. Rougieux, and D. Macdonald, *Phys. Status Solidi RRL* **10**, 443–447 (2016).
- <sup>13</sup>J. Mullins *et al.*, in *ICDS-29 Technical Digest* (2017), p. 31.
- <sup>14</sup>E. N. Sgourou, T. Angeletos, A. Chroneos, and C. A. Londos, *J. Mater. Sci.: Mater. Electron.* **27**, 2054 (2016).
- <sup>15</sup>K. L. Brower, *Phys. Rev. B* **26**, 6040 (1982).
- <sup>16</sup>N. Inoue, Y. Goto, T. Sugiyama, H. Seki, K. Watanabe, and Y. Kawamura, *Solid State Phenom.* **205–206**, 228 (2013).
- <sup>17</sup>N. Inoue, Y. Goto, H. Seki, K. Watanabe, H. Oyama, and Y. Kawamura, *Phys. Status Solidi C* **9**, 1931 (2012).
- <sup>18</sup>H. Sawada and K. Kawakami, *Phys. Rev. B* **62**, 1851 (2000).
- <sup>19</sup>H. Kageshima, A. Taguchi, and K. Wada, *Physica B* **340–342**, 626 (2003).
- <sup>20</sup>J. P. Goss, I. Hahn, R. Jones, P. R. Briddon, and S. Oeberg, *Phys. Rev. B* **67**, 045206 (2003).
- <sup>21</sup>F. S. Karoui and A. Karoui, "Application of quantum mechanics for computing the vibrational spectra of nitrogen complexes in silicon nano-materials," in *Some Applications of Quantum Mechanics* (Intech, Croatia, 2012).
- <sup>22</sup>H. J. Stein, "Nitrogen in crystalline Si," in *Symposium K—Oxygen, Carbon, Hydrogen and Nitrogen in Crystalline Silicon* (Mater. Res. Soc. Symp. Proc., 1985), Vol. 59, p. 523.
- <sup>23</sup>H. J. Stein, *Appl. Phys. Lett.* **52**, 153 (1988).
- <sup>24</sup>N. Inoue, M. Nakatsu, K. Tanahashi, H. Yamada-Kaneta, H. Ono, C. D. Akhmetov, O. Lysytskiy, and H. Richter, *Solid State Phenom.* **108–109**, 609 (2005).